Observations from moorings in the Aleutian Passes: temperature, salinity and transport

P. J. STABENO,[1,*] D. G. KACHEL[1], N. B. KACHEL[2] AND M. E. SULLIVAN[2]

[1]*NOAA/Pacific Marine Environmental Laboratory, 7600 Sand Point Way NE, Seattle, WA 98115-6349, USA*
[2]*JISAO/UW, 7600 Sand Point Way NE, Seattle, WA 98115-6349, USA*

ABSTRACT

Between May 2001 and September 2003, a series of moorings were deployed in four of the Aleutian Passes – Tanaga Pass (12 months of data), Akutan Pass and Seguam Pass (18 months), and Amukta Pass (36 months). Instruments on each mooring measured temperature, salinity and current velocity. Tidal currents dominated the flow in each pass, including a strong fortnightly component in the three deeper passes (Tanaga, Seguam, and Amukta). Net transport in each of the passes was northward, varying from 0.1×10^6 m^3 s^{-1} in Akutan Pass and 0.4×10^6 m^3 s^{-1} in Seguam to $>4.0 \times 10^6$ m^3 s^{-1} in Amukta Pass. The transport in Amukta Pass, calculated from current meters, was approximately five times as large as previously estimated from hydrographic surveys. At monthly and longer periods, the variability in transport in Amukta Pass was related to the position and strength of the Alaskan Stream southeast of the pass. Vertical mixing was examined in Akutan and Seguam Passes. Strong tidal currents mix the water column top-to-bottom over the shallow sills in the passes, a depth of 80 m in Akutan and 140 m in Seguam Pass, providing a critical source of nutrients to the Bering Sea ecosystem.

Key words: Aleutian Passes, Bering Sea, currents, mixing, tides, transport

INTRODUCTION

The Aleutian Arc stretches ~3000 km from the tip of the Alaskan Peninsula to the Kamchatka Peninsula (Fig. 1). The arc, with its numerous passes, forms a porous boundary between the North Pacific and the Bering Sea. The character of the passes that cut through the arc changes from the narrow, eastern-most False Pass to the broad, deep, western-most Kamchatka Strait. The eastern passes (e.g. Unimak, Akutan and Umnak Passes) are shallow (sill depth <100 m) and narrow (<20 km). West of Samalga Pass (~170°W), deeper (>400 m) passes such as Amukta and Amchitka occur. Farther west beyond the date line, the deepest passes (Near Strait and Kamchatka Strait) can be found. In addition to variation in depth, the north–south width of the shelf associated with the Aleutian Arc narrows from east to west, with the greatest north–south extent (>80 km) occurring east of Samalga Pass.

Three major currents (Fig. 1) dominate the flow in this region: the Alaska Coastal Current (ACC) and Alaskan Stream in the North Pacific, and the Aleutian North Slope Current (ANSC) in the Bering Sea (Favorite *et al.*, 1976; Stabeno *et al.*, 1999). On the North Pacific shelf east of Samalga Pass, the remnants of the ACC flow southwestward along the shelf and through the eastern passes (Stabeno *et al.*, 1995; Stabeno *et al.*, 2004). The ACC, a wind-driven current with a prominent fresh core, originates ~1000 km to the east along the coast of the Alaskan panhandle. The average transport of the ACC in the vicinity of Kodiak Island exceeds 1.2×10^6 m^3 s^{-1}, but, by the time it reaches Unimak Island, it is reduced by approximately 75% through loss of water due to off-shelf flux, interaction with topography and friction (Stabeno *et al.*, 2002). Its baroclinic structure, however, with its prominent freshwater core is still clearly evident at Unimak Pass. Flowing southwestward along the shelf break is the Alaskan Stream, the western boundary current of the eastern portion of the subarctic gyre. This narrow (<100 km), deep (>5000 m), high-speed current transports $>20 \times 10^6$ m^3 s^{-1} southwestward along the south side of the Aleutian Arc. Portions of the Alaskan Stream flow northward through the passes forming the ANSC, the narrow, high speed current that flows northeastward along the north slope of the Aleutian Islands (Reed and Stabeno, 1994).

It has been known for several decades that the ACC flows northward through Unimak Pass onto the

*Correspondence. e-mail: phyllis.stabeno@noaa.gov
Received 19 December 2003
Revised version accepted 20 August 2004

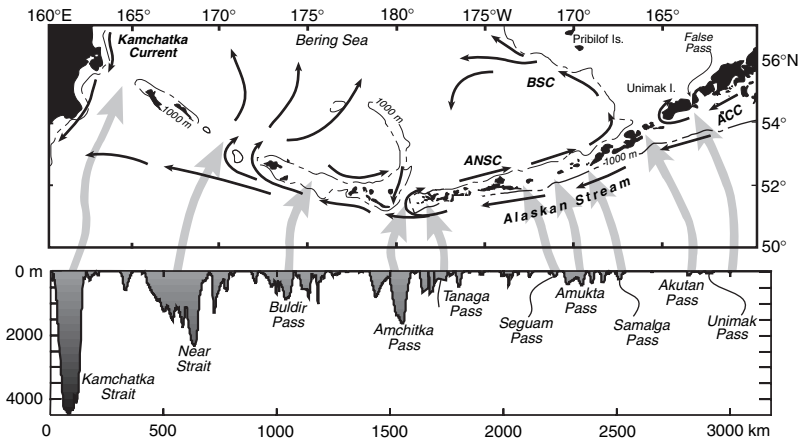

Figure 1. The mean circulation along the Aleutian Arc is shown together with geographic place names. The lower panel shows the depth of the passes in the Aleutian Arc.

Bering Sea shelf (Schumacher *et al.*, 1982; Stabeno *et al.*, 2002). It was thought that the last remnant of the ACC flowed through Unimak Pass and that no coherent signal of the current occurred to the west of the pass. What has been more recently hypothesized (Ladd *et al.*, 2005a) is that some portion of the ACC continues southwestward along the Aleutian Arc, flowing northward through passes as far west as Samalga Pass, and that the freshwater from the ACC can be seen along the north side of the Aleutians (Ladd *et al.*, 2005a) and in the ANSC (Stabeno and Reed, in review).

The northward flow through the passes supplies an important source of nutrients, heat and salts for the Bering Sea ecosystem (Favorite, 1974; Stabeno *et al.*, 1999). To date, the magnitude of transport through the Aleutian Passes has primarily been estimated through geostrophic calculations, although a few current records do exist in some of the passes. Northward flow through Amukta Pass, the eastern most of the larger passes, has an estimated geostrophic transport of $\sim 1.0 \times 10^6$ m^3 s^{-1} (Reed and Stabeno, 1997). Southward flow also occurs through the pass, typically on the western side, with a transport of $\sim 0.4 \times 10^6$ m^3 s^{-1}, resulting in a net northward geostrophic transport of $\sim 0.6 \times 10^6$ m^3 s^{-1}. Fewer hydrographic transects have been made across Amchitka Pass (Fig. 1), but a similar spatial pattern dominates (northward flow typically on the east side of the pass and southward on the west; Stabeno *et al.*, 1999). The magnitude of observed transport at this pass ranges from a net southward transport of 2.8×10^6 m^3 s^{-1} (consisting of northward transport of 1.6×10^6 m^3 s^{-1} and southward transport of 4.4×10^6 m^3 s^{-1}) to a net northward transport of 4.0×10^6 m^3 s^{-1} (6.1×10^6 m^3 s^{-1} northward and 2.1×10^6 m^3 s^{-1} southward). A single, year-long current meter mooring was deployed in 1989 at the northern end of Amchitka Pass and provided a rough estimate of transport of $2–3 \times 10^6$ m^3 s^{-1} into the Bering Sea (Reed, 1990). Flow in Near Strait, the second deepest pass in the Aleutian Arc, is northward and has been estimated to exceed 10×10^6 m^3 s^{-1}, although there are relatively few measurements (Stabeno *et al.*, 1999). The only significant pass with net southward flow is Kamchatka Strait. Here, the Kamchatka Current, the western boundary current of the cyclonic Bering Sea gyre, flows southward (Stabeno *et al.*, 1999). This western-most strait is the deepest of the passes and while the net transport is southward (estimated $>12 \times 10^6$ m^3 s^{-1}), the flow on the eastern side, particularly near the bottom, is northward. This northward bottom flow is the source of the deep water (>2000 m) of the Bering Sea (Reed and Mordy, 1999).

It must be noted that these transports are only approximations, since few measurements have been made with moored arrays. One exception to this is Unimak Pass (Fig. 1), where nearly 3 years of data were collected from moored current meters. While the total transport is northward and estimated at 0.3×10^6 m^3 s^{-1}, approximately one third of this flow is barotropic (Stabeno *et al.*, 2002). In addition, there is a strong correlation between the alongshore winds and the barotropic transport through Unimak Pass.

Since 2001, a series of moorings have been deployed in some of the eastern and central passes (those east of Amchitka Pass). Specifically, moorings were deployed at a total of 10 sites (Fig. 2), two each in Akutan Pass (18 months), Seguam Pass (18 months) and Tanaga Pass (12 months); in addition, a series of moorings was deployed at four sites in Amukta Pass (30 months). The purpose of these moorings was to obtain estimates of transport through the passes, mixing processes within the passes, time series of temperature and salinity within the passes, and an understanding of the dynamics that control flow

Figure 2. The locations of the moorings discussed in this article are shown as open triangles. The bathymetry of Tanaga, Seguam, and Akutan Passes are shown in detail with the positions of the moorings indicated once again as open triangles. The moorings in Amukta Pass are numbered right to left, with Amukta-1 in the east and Amukta-4 in the west.

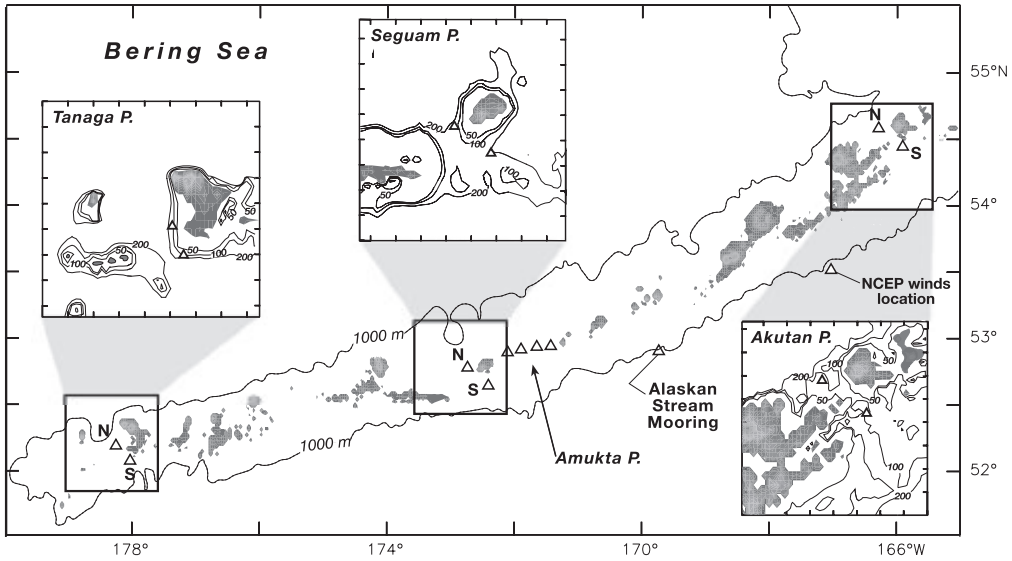

through the passes. Measurements made at these moorings are the focus of this article.

After the discussion of data and methods, we will explore the transport through and water properties in each of the four passes, beginning with the smallest (Akutan) and ending with the largest (Amukta). We then examine mixing in the passes as evident in the temperature records. Finally, we discuss the importance of the passes to the productivity of the Bering Sea. Since few measurements of currents have been made in the passes, a primary purpose of this paper is to present the large data set that has been collected.

DATA AND METHODS

Mooring design

In May 2001, subsurface moorings were deployed in Akutan, Amukta, and Seguam Passes (Fig. 2). In both Akutan and Seguam Passes, two moorings (one at the north end of each pass and the second at the south end) were deployed, while in Amukta Pass, four moorings were deployed east–west across the pass. All moorings were taut-wire moorings. The southern mooring in Seguam Pass contained a 300 kHz acoustic Doppler current profiler (ADCP), a nitrate meter (discussed in Mordy *et al.*, 2005) and a SeaBird MicroCat (microcat) to measure temperature and salinity. The ADCP was mounted 15 m above the bottom and the microcat 10 m above the bottom. The northern mooring contained an Aanderaa RCM-9, an acoustic current meter (15 m above the bottom) and a microcat (13 m above the bottom). The southern mooring in Akutan Pass contained a RCM-9 (15 m above the bottom) and a microcat (13 m above the bottom), while the northern mooring contained a 300 kHz ADCP (15 m above the bottom), and a microcat to measure temperature and salinity (13 m above the bottom). All four moorings in Amukta Pass were designed the same, with a 75 kHz ADCP (10 m above the bottom) and a microcat (6 m above the bottom). The plan for recovery and deployment was the same at each of these eight mooring sites. Initial deployment occurred in May 2001, and moorings were turned around (recovered and new, identical moorings deployed) in September 2001 and May 2002. In October 2002, the moorings in Seguam Pass and Akutan Pass were recovered for the final time. The four Amukta moorings were turned around in October 2002, May 2003 and in October 2003. On three occasions, releases failed and moorings were recovered later by dragging or by ROV without loss of data.

In May 2002, two moorings (one in the northern part of the pass and a second in the southern part) were deployed in Tanaga Pass (Fig. 2). They remained in the water for 1 year and were recovered the following May. The northern mooring contained a 300 kHz ADCP and a microcat to measure temperature and salinity. The ADCP was mounted 15 m above the bottom and the microcat 13 m above the bottom. The southern mooring contained a RCM9

(15 m above the bottom) and a microcat (13 m above the bottom).

In addition to measuring flow and water properties near the bottom in these passes, an understanding of mixing throughout the water column was desired. So in May 2002, two moorings were deployed to measure temperature at several depths in the water column. The first mooring was a modification of the northern Akutan mooring. In addition to the ADCP and microcat, three thermistors were deployed at 15, 35, and 55 m below the surface. A second mooring was deployed ~500 m from the southern mooring in Seguam Pass. This mooring had six thermistors at 20 m separation (30, 50, 70, 90, 110, and 130 m below the surface). In October 2002, shortly before it was recovered, this mooring lost its flotation (including the top instrument) because of the strong currents (>250 cm s^{-1}) in the pass. The remaining instruments were recovered later using a ROV.

Data from a mooring in ~1000 m of water in the Alaskan Stream southeast of Amukta Pass are also presented (Fig. 2). This was a taut-wire mooring with an upward looking 75 kHz ADCP at ~500 m depth. This mooring was deployed in May 2001 and recovered in May 2002, providing 1 year of current measurements.

Calculations and processing

The ADCPs measured velocity at hourly intervals throughout the water column. The bin size varied among instruments and is presented in Table 1. The microcats collected temperature and conductivity (salinity) hourly, although a few thermistors collected data at 10-minute intervals. Both hourly and 6-hourly data are presented in this manuscript. All 6-hourly data were obtained by filtering the raw data using a low-pass 35 h, cosine-squared tapered Lanczos filter to remove diurnal and semi-diurnal tidal signals, and the data were then re-sampled at 6-hour intervals.

Table 1. Locations of the moorings and statistics of the current records.

Mooring	Location (Latitude, Longitude)	Bottom depth (m)	Measurement depth (m)	Net speed, direction (cm s^{-1}, °T)	Principal axis (°T)	Maximum speed (cm s^{-1})
Akutan north	53.93°N, 166.30°W	~80	14	6 (~300°)	300° (79%)	183
	Bin size: 2 or 4 m		42	6 (~280°)	300° (~73%)	168
			62	4 (~215°)	300° (~65%)	145
Akutan south	54.07°N, 165.92°W	~90	75	12 (~350°)	340° (~65%)	139
Seguam north	52.27°N, 172.75°W	160	145	20 (~0°)	305° (~68%)	216
Seguam south	52.13°N, 172.42°W	165	150	15 (~0°)	69° (~81%)	257
	Bin size: 4 m		81	18 (~6°)	60° (~74%)	212
			141	15 (~1°)	40° (~75%)	170
Amukta-1	52.43°N, 171.45°W	410	75	45 (349°)	342° (67%)	224
	Bin size: 10 m		180	50 (344°)	16° (60%)	246
			390	22 (350°)	350° (93%)	168
Amukta-2	52.42°N, 171.66°W	460	75	10 (1°)	347° (60%)	242
	Bin size: 8 or 10 m		180	7 (51°)	344° (56%)	255
			430	13 (70°)	75° (67%)	134
Amukta-3	52.60°N, 171.93°W	310	75	13 (2°)	355° (75%)	233
	Bin size: 8 or 10 m		180	11 (0°)	342° (63%)	208
			280	4 (333°)	39° (65%)	141
Amukta-4	52.38°N, 172.12°W	370	75	9 (~35°)	14° (~70%)	207
	Bin size: 8 or 10 m		180	8 (~235°)	350° (~70%)	203
			325	8 (~255°)	30° (~65%)	134
Tanaga north	51.66°N, 178.25°W	187	62	25 (344°)	348° (86%)	192
	Bin size: 4 m		82	24 (348°)	339° (88%)	205
			162	19 (341°)	330° (92%)	166
Alaskan stream	52.39°N, 169.75°W	986	55	43 (254°)	78° (80%)	159
	Bin size: 10 m		180	35 (251°)	71° (90%)	145
			450	6 (253°)	86° (87%)	66

While the moorings were deployed as close as possible to the same position, there was some variation in location. The location, bottom depth and depth of the measurement are all averages. The positions were all within 2 km, and the bottom depth varied by less than 5 m. The depth of measurements varied by as much as 2 m in the shallow passes and 5 m in Amukta Pass. The maximum speed was calculated using hourly time series. Net speed and principle axis were calculated from low-pass filtered data.

Hydrographic casts were done at deployment and recovery to help ground truth the temperature and salinity data. All instruments were calibrated yearly.

The ADCPs provided excellent data return; only one instrument failed to collect data and that was during the sixth deployment cycle in Amukta Pass. Because of that, only 2 years of current data are presented from that pass, although 2.5 years of temperature and salinity are discussed. One consistent problem with the 75 kHz ADCPs was the loss of data in the upper water column. This problem was particularly egregious at the eastern-most Amukta site, where gaps of 2 days occurred to a depth 90 m on ~10 occasions per year. Longer gaps were less common and occurred typically to a depth of less than 60 m. The likely cause was the lack of particles (reflectors) in the upper water column, resulting in low signal-to-noise ratio. While small gaps were filled through spectral techniques, larger (>48 h) gaps were left unfilled except for the calculations of transport. Here, data were extrapolated upward. Estimates of transport were obtained at Amukta Pass using the northward component of the currents, which is normal to the line of moorings lying east-west across the pass. The northward velocity in each ADCP bin was multiplied by the cross-sectional areas. These were then summed, providing a time series of transport through the pass. This method was successfully employed previously to obtain time series of transport in Shelikof Strait (Stabeno *et al.*, 1995).

RESULTS

Akutan Pass

Akutan Pass, the eastern-most pass discussed in this manuscript, is shallow (sill depth ~60 m) and narrow (~10 km). The bathymetry is complex with a broad (>40 km) shelf on the south side of the pass and a narrower shelf to the north (Fig. 2). On the south side, a trough (>100 m deep) cuts into the shelf eventually shoaling to ~60 m near the centre of the pass. The mooring sites were ~20 km apart, with the northern site in ~85 m of water and the southern site in ~90 m (Table 1).

A strong seasonal signal is evident in both near-bottom temperature time series, with maximum temperatures occurring in September and minimum temperatures in February (Fig. 3). During summer, temperatures were more variable at the northern site than at the southern site. While the maximum temperatures were similar at the two locations, the minimum temperatures were ~1°C cooler at the northern site. During winter, near-bottom temperatures were similar at the two locations.

The near-bottom salinity records, however, were markedly different, with the northern location more saline (~0.4 psu) and more variable on fortnightly and shorter time scales than the southern station. From May to August of both 2001 and 2002, the salinity at the southern site was relatively stable at ~32.4 psu, but during autumn and winter three, month-long

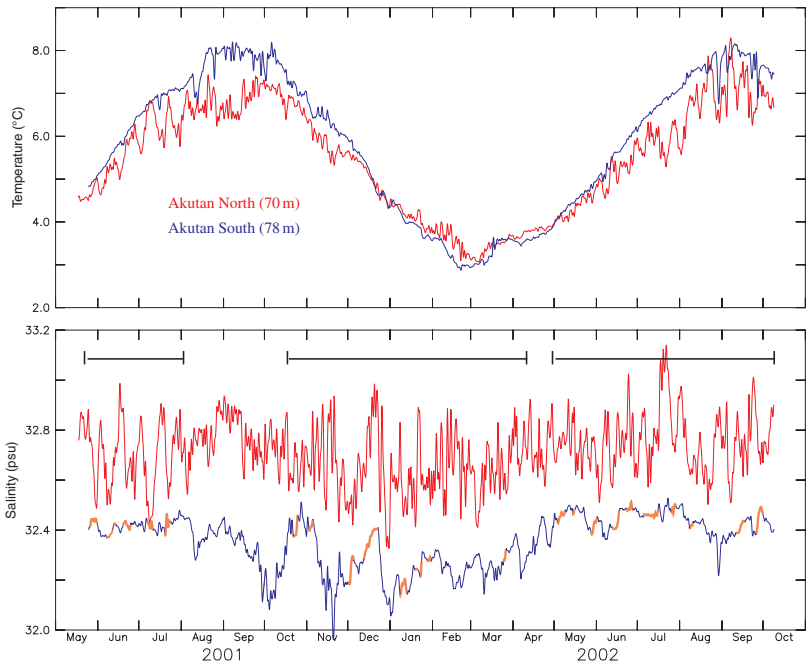

Figure 3. Low-pass filtered time series of temperature (upper panel) and salinity (lower panel) at the two mooring locations in Akutan Pass. The orange portion of the blue salinity line indicates periods when the flow was southward (see Fig. 4). The solid lines at the top of the salinity panel indicate when the current data was successfully collected. The average depth of the measurements is indicated.

pulses of lower salinity (32.0 psu) occurred. The maximum salinities at the southern mooring were similar to those measured south of Unimak Pass in 1996–1997 (Stabeno *et al.*, 2002), but the three pulses of fresher water that occurred in Akutan Pass were more saline than pulses that have been observed at Unimak Pass (~31.6 psu). At Unimak Pass, freshening of the water column begins in October, with the least saline water appearing in January. This is consistent with the timing of increased freshwater run-off that occurs in the coastal, eastern Gulf of Alaska. Maximum run-off occurs in early autumn, and this freshwater core is advected southwestward in the ACC, reaching Unimak Pass several months later. Thus, the timing of the appearance of freshwater at Akutan Pass is consistent with the hypothesis that a portion of the ACC continues past Unimak Pass and flows through Akutan Pass.

Tidal currents dominate the velocity in Akutan Pass. While maximum velocity of the low-pass filtered data was ~50 cm s^{-1} (Fig. 4), the maximum speed of the hourly data exceeded 160 cm s^{-1} at both sites. Tides were dominated by the principal lunar semi-diurnal constituent (M_2) component (amplitude of the major axis ~38 cm s^{-1}), which was largely barotropic at the northern site from ADCP measurements. The luni-solar diurnal constituent (K_1) was weaker than the semi-diurnal (amplitude of major axis 14 cm s^{-1}).

The low frequency near-bottom currents at the two sites differed markedly (Fig. 4). At the northern location, the mean flow at 59 m was northward, but this was primarily a result of pulses of strong northward flow; more typically the flow was weakly southward (~10 cm s^{-1}). These long periods of southward flow were likely due to the position of the mooring on the west slope of the pass, where a weak, southward flow of Bering Sea water into the pass occurred. In contrast at 22 m, the flow is stronger and predominately northward (Fig. 4).

The flow was stronger at the southern mooring site than at the northern sites and predominantly northward, although periodically it was punctuated by short periods (1–7 days) of southward flow. When currents are examined in conjunction with salinity, this southward flow is often (although not always) associated with increasing salinity (the orange portion in the blue salinity line, lower panel Fig. 3). This pattern was similar to that observed in Unimak Pass (Stabeno *et al.*, 2002). Thus, fluctuations in the near-bottom salinities are associated at least in part with the direction of flow – southward flow from the Bering Sea is more saline than northward flow from the North Pacific. The bottom currents at Unimak Pass were significantly correlated with the alongshore winds (Schumacher *et al.*, 1982; Stabeno *et al.*, 2002), with strong flow from North Pacific into the Bering Sea occurring during periods when the alongshore winds confined the freshwater of the ACC along the Alaskan Peninsula. This was not the case at Akutan; the bottom currents were not correlated with local winds. This indicates that, while the freshwater that flows through Akutan Pass may have remnants of the ACC, the ACC is no longer an organized, wind-driven flow, and other mechanisms rather than winds determine the magnitude of northward flow through the pass.

Seguam Pass

Seguam Pass, ~300 km west of Akutan Pass, is deeper (>120 m) and wider (east–west), with a shorter along-axis (north–south) shelf width than at Akutan Pass.

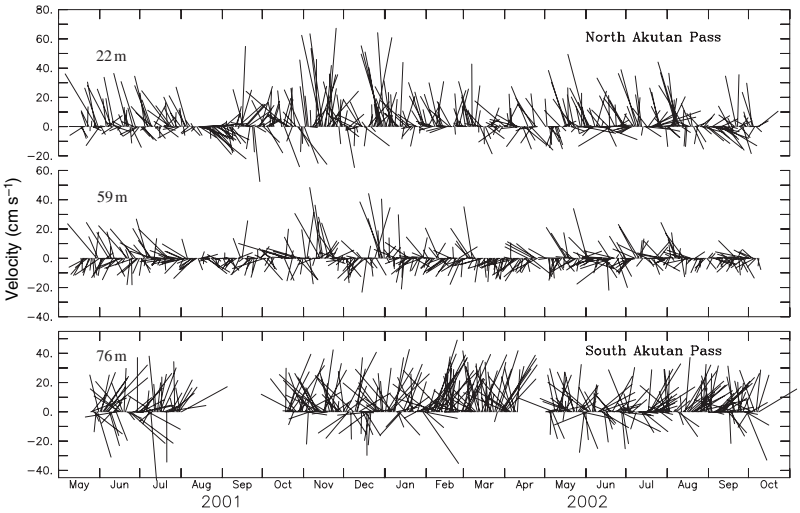

Figure 4. Low-pass filtered time series of currents in Akutan Pass. Currents were measured by ADCPs at the northern site. All records have been rotated 320°T. The average depth of the measurements is indicated.

At first glance, the bathymetry appears less complex than at Akutan Pass (Fig. 2), but that is primarily an artifact of the bathymetry–Seguam is deeper and thus lacks the small-scale complexity of the 50 m isobath. The two mooring sites were ~20 km apart, with the northern mooring site in ~160 m and the southern mooring site at 165 m (Table 1).

There was not a strong annual temperature signal at the northern site in Seguam Pass (Fig. 5). There was, however, a well-defined annual signal at the southern site with an amplitude of ~0.5°C, with the warmest temperatures occurring in late September in both years. Even though the instruments were at similar depths, low-pass filtered, near-bottom temperatures at the southern site were consistently warmer than those at the northern site. At both sites, fluctuations (~0.4°C) occurred at fortnightly time scales. These are especially evident in the summers. This variability in the low-pass filtered data at the southern site was related to variability in the currents, with increases in temperature associated with stronger northward flow. Interestingly, a number of increases in temperature at the southern site are associated with decreases in temperature at the northern site (Fig. 5, arrows). This is caused by a difference in the tidal cycles at the two sites and is discussed below. Near-bottom salinity at the northern site was higher than at the southern site. The amplitudes of the fluctuations in the two salinity time series are similar (0.2 psu). Thus, the Bering Sea end of the pass was characterized by cooler, more saline water than the southern side.

Once again, currents were dominated by tides. At the southern site, the mean currents were <20 cm s^{-1}, but the maximum velocity often exceeded 200 cm s^{-1}. The dominant tidal constituent was K_1 with an amplitude of the major axis ranging from 70 cm s^{-1} near the bottom to >100 cm s^{-1} near the surface. In contrast, the amplitude of the M_2 was less than half that of K_1, ranging from 25 cm s^{-1} near the bottom to slightly larger than 40 cm s^{-1} near the surface. At the northern site, the near-bottom amplitudes of K_1 and M_2 are almost identical at 60 cm s^{-1}.

Differences in the tidal cycles at the two sites result in differences in the temperature at the northern and southern sites, as can be seen in time series of the hourly data (Fig. 6). Time series of temperature appear almost out of phase at the two sites (Fig. 6, second panel). Cooler water at the northern site is punctuated with periods of warmer water during strong northward flow (Fig. 6, third panel). In contrast, temperatures are warmer at the southern site and punctuated by periods of cooler water associated with southward flow (Fig. 6, bottom panel). The lag between the responses of the temperature to changes in north–south flow is associated with how long it takes to advect North Pacific (Bering Sea) water northward (southward) through the pass. So, the lack of correlation between temperature (or salinity) at sites north or south of the sill is caused by local differences in the currents.

The character of low-pass filtered currents at Seguam Pass (Fig. 7) differed markedly from those at Akutan Pass (Fig. 4). At both sites in Seguam Pass, the low-pass filtered flow was persistently northward, from the North Pacific into the Bering Sea, with few reversals. While the northern record is unfortunately short because of instrument failures; it appears consistently stronger than that observed at the southern site. This is likely a result of the sharper slope in bathymetry at the northern location, which intensifies the flow. An examination of the nearly continuous times series from the southern site gives an indication of stronger currents during the winter, or at least episodes of stronger flow. Throughout the record a fortnightly signal is evident, although it is clearest in May through October of 2002. Such a fortnightly signal is also evident in the salinity records and, to a lesser extent, in the temperature records (Fig. 5).

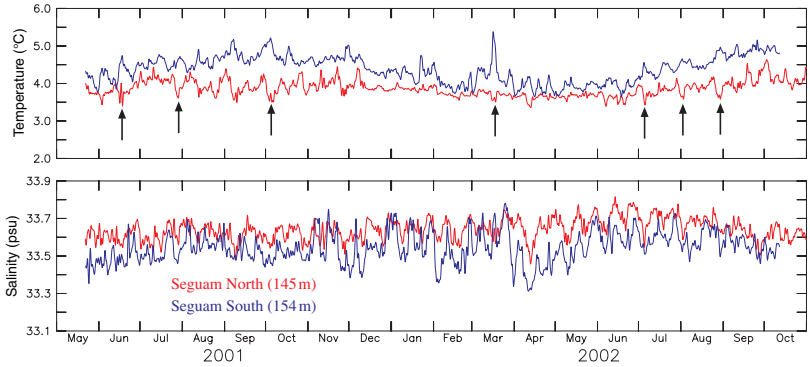

Figure 5. Low-pass filtered time series of temperature (upper panel) and salinity (lower) panel at the two mooring locations in Seguam Pass. The average depth of the measurements is indicated. Arrows indicate periods when temperature increases at the southern site were associated with temperature decreases at the northern site.

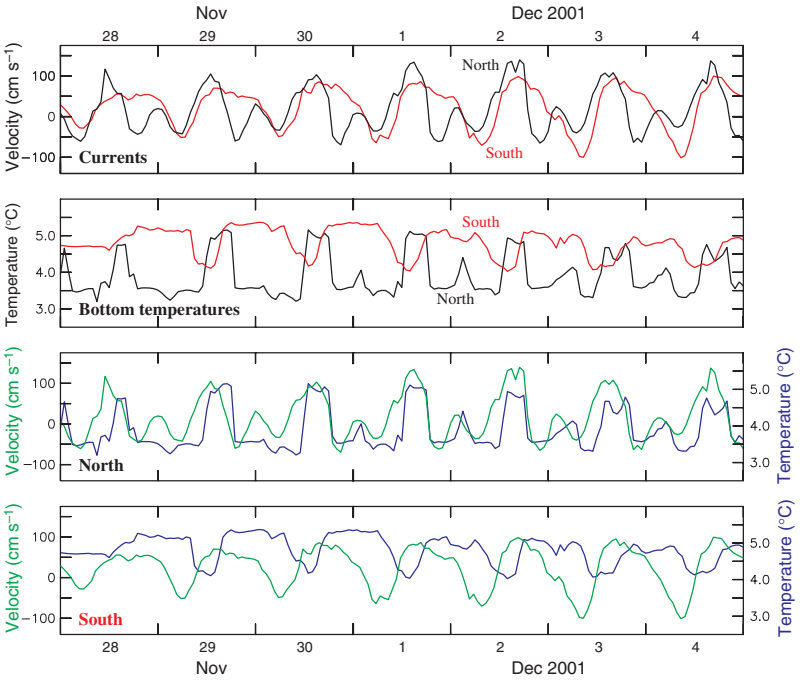

Figure 6. Hourly northward velocity and temperature measured at Seguam Pass. The top panel is a comparison of northward currents at the two locations. The second panel is a comparison of temperature at the two sites. The third and fourth panels compare temperature and northward near-bottom velocity at the northern and southern sites.

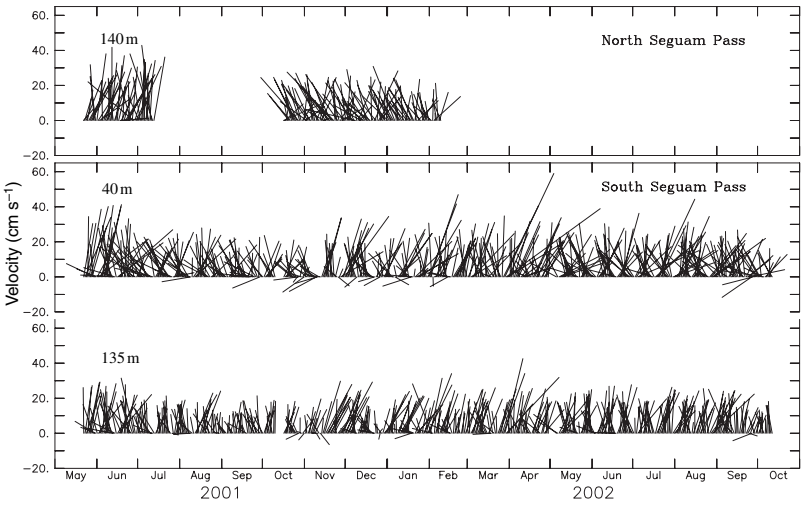

Figure 7. Low-pass filtered time series of currents at Seguam Pass. Currents were measured by ADCPs at the southern site. The records are not rotated. The average depth of the measurements is indicated.

Tanaga Pass

Tanaga Pass, ~300 km farther west along the Aleutian Arc, is at the western edge of a large plateau lying at ~500 m below the sea surface (Fig. 2). Several islands rise up from the plateau forming passes between them. Tanaga Pass is both deeper (sill depth ~210 m) and wider than Seguam Pass. Because of its greater distance from the other moorings (and hence greater commitment of ship time), both moorings in Tanaga Pass were deployed for 1 year, rather than the ~6-month deployment that was used in the other passes. Once again two sites were chosen, one on the northern side of the 210 m sill and the other ~10 km to the south. The moorings were deployed along the eastern side of the pass, rather than near the centre. While an attempt was made to deploy each of the moorings at similar depths, at Tanaga Pass the depths of sites differed by >30 m, with the northern site being deeper (Table 1).

Probably because of the close proximity of the mooring sites, temperatures at the two sites were remarkably similar, especially from December through April (Fig. 8). During autumn, the bottom tempera-

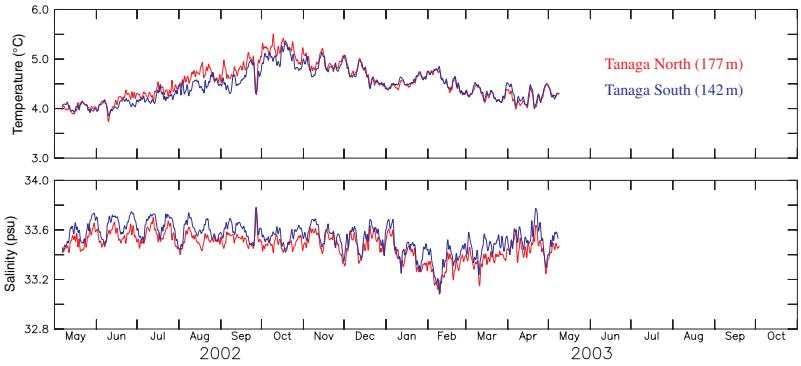

Figure 8. Low-pass filtered time series of temperature (upper panel) and salinity (lower) panel at the two mooring locations in Tanaga Pass. The average depth of the measurements is indicated.

ture at the northern site was slightly warmer than that at the southern site, even though it was deeper than the southern instrument. A well-defined annual signal is evident in both temperature time series, with the maximum temperature occurring in October. Unlike at the other two passes, the salinity time series at Tanaga Pass were highly correlated, with the southern site more saline. Both records show a well-defined fortnightly signal, especially in May to December. Thus the water at the southern site was cooler and more saline than that at the northern site, which is opposite of what occurred at Akutan and Seguam Passes. There is not enough data to know why this occurred, but one possibility is that there is less mixing at this site because Tanaga is deeper than Seguam Pass.

Once again, the tidal amplitudes were larger than the mean currents (Table 1). At the northern sites, the semi-diurnal M_2 varies from ~55 cm s^{-1} near the surface to ~35 cm s^{-1} near the bottom. The K_1 constituent is weaker than M_2, varying from ~25 cm s^{-1} near the surface to ~35 cm s^{-1} near the bottom.

The low-pass filtered currents at the northern site (Fig. 9) were similar in character to those that were measured at Seguam Pass (Fig. 7), with strong flow from the North Pacific into the Bering Sea with few reversals. Vertically, currents were highly correlated, with more frequent and stronger reversals in the upper water column than occurred near the bottom. There also is an indication of variability in the direction and strength of the vectors at fortnightly frequencies. Unfortunately, the current meter at the southern site malfunctioned.

Amukta Pass

Amukta Pass is wider (~80 km east-west) and deeper (>400 m) than the other three passes discussed. While much larger than the small passes, it is far smaller than the major passes of Kamchatka Strait, Near Strait and Amchitka Pass (Fig. 1). Because of the east–west width of the pass, it was inappropriate to deploy moorings north-south in the pass. Instead, we placed moorings at four locations, ~14 km apart, east–west across the pass to examine spatial variability. Of the four moorings, Amukta-1 is the eastern site and Amukta-4 is the western site in the pass.

The envelope of variability of the near-bottom temperatures for the 2.5-year period was ~1°C (Fig. 10). The annual cycle evident in all four bottom-temperature records is surprising given the depths of the instruments (300–450 m). Maximum temperatures occurred in January while minimum temperatures occurred in late April or May. The most marked cooling occurred in early 2002, when the bottom temperatures cooled by ~1°C in a 4-month period. The time series of near-bottom salinity differed in a consistent pattern across the pass, with the highest salinity occurring on the eastern side of the pass and lowest salinity on the western side. This was not purely a reflection of the depth of the instruments, since the deepest mooring was Amukta-2 and

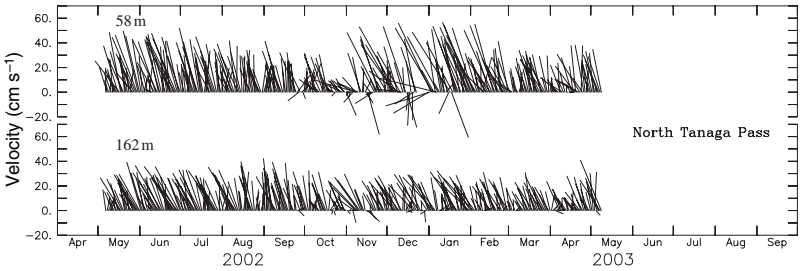

Figure 9. Low-pass filtered time series of currents at two depths in Tanaga Pass at the northern mooring site. The velocity vectors have not been rotated. The average depth of the measurements is indicated.

Figure 10. Low-pass filtered time series of near-bottom temperature (upper three panels) and salinity (lower three panels) at the four mooring sites in Amukta Pass. The average depth of the measurements is indicated.

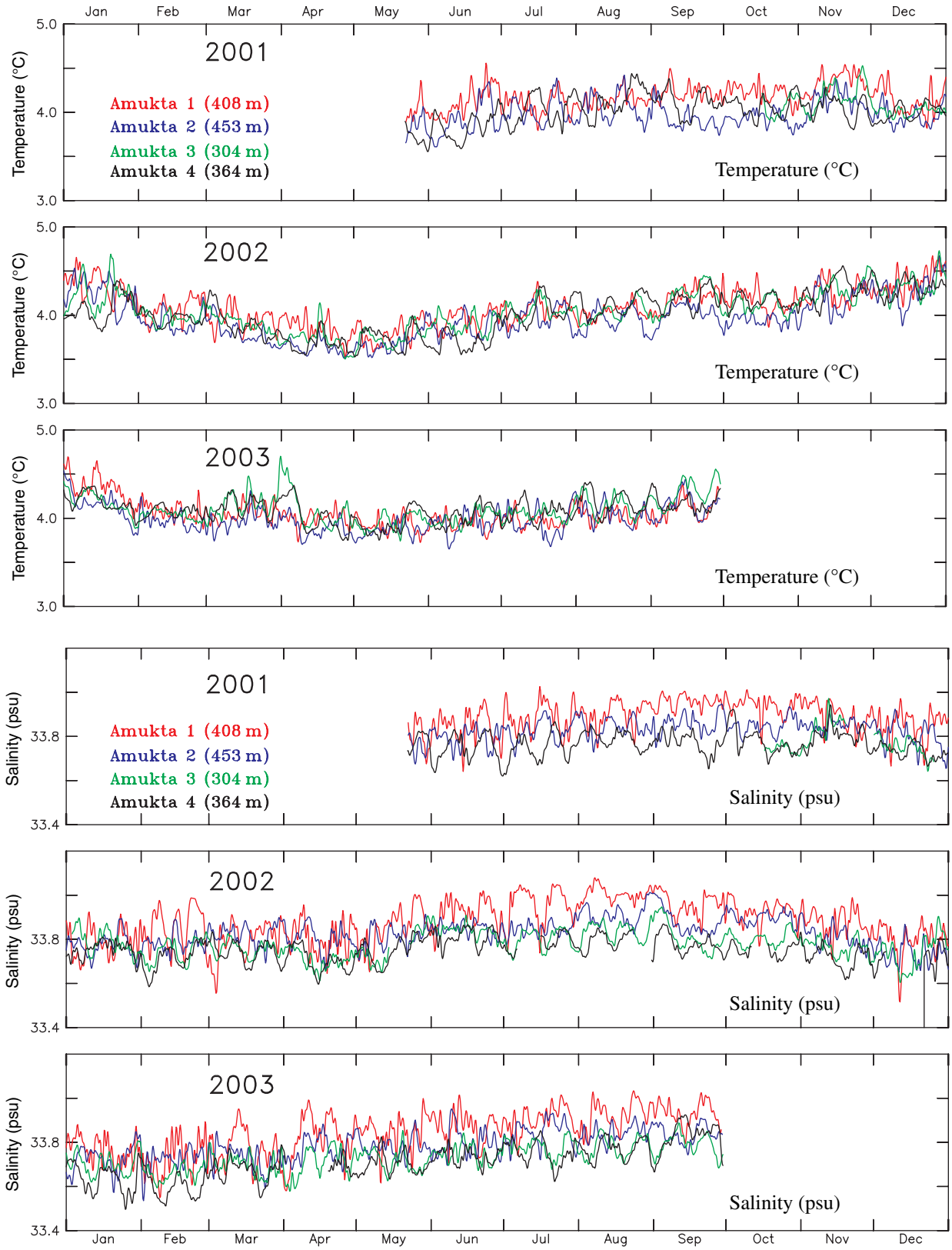

the shallowest Amukta-3. The higher salinity at Amukta-1, as compared to Amukta-2, indicates that the isopycnals in the lower part of the water column consistently sloped downward toward the eastern side of the pass, reflecting northward baroclinic flow there. Each of the sites showed evidence of a strong fortnightly signal that caused variations in salinity of as much as 0.2 psu at Amukta-1 and lesser amounts at the other locations.

As in the other passes, tidal currents dominate the velocity field, playing an important role in mixing. The semi-diurnal M_2 is stronger on the eastern side of the pass and weaker on the western side (Fig. 11). The diurnal K_1 is just the opposite, stronger on the west and weaker on the east. The largest tidal amplitudes were in the upper half of the water column and decreased with depth.

Time series of low-pass filtered currents are shown at the four mooring sites. They differ in character from east to west (Fig. 12). Along the eastern side of Amukta Pass, the flow was strongly toward the north, with no reversals at depth and few near the surface. At Amukta-2, the flow was variable in both speed and direction except near the bottom, where the flow was eastward, likely a result of bathymetric steering. At the next site, Amukta-3, the flow was weaker, but more organized than at Amukta-2. This was the shallowest site and the currents at the bottom were near zero in strength. Finally, the western-most site had southward flow throughout the water column. The strong northward flow along the eastern side of the pass is associated with higher, near-bottom salinities, while the southward flow along the western edge of the pass is associated with lower salinities, even though the western instrument was >50 m deeper than Amukta-3.

A composite of average north–south flow through Amukta Pass shows a strong northward jet on the east of side of the pass and weak southward flow on the west side (Fig. 11). Interestingly, on both the eastern and western slope of the passes, the maximum mean current was subsurface.

The salinity (Fig. 10) and velocity (Fig. 11) time series both show temporal variability at fortnightly frequencies. From examination of current spectra, there was a strong peak at 13.7 days. We removed the annual signal in the current velocities and fit sines and cosines at a frequency of the lunar fortnightly tide (Mf, 13.66 days) to the low-pass filtered northward velocities at each of mooring sites. While the sine waves did not fit the shape of the wave exactly, the amplitudes formed a consistent pattern throughout the water column. Tidal amplitudes of the fortnightly signal were largest at the surface and weakest in the mid-water (Fig. 11).

Transport

One of the primary purposes of the mooring array was to determine the transport through the passes. The

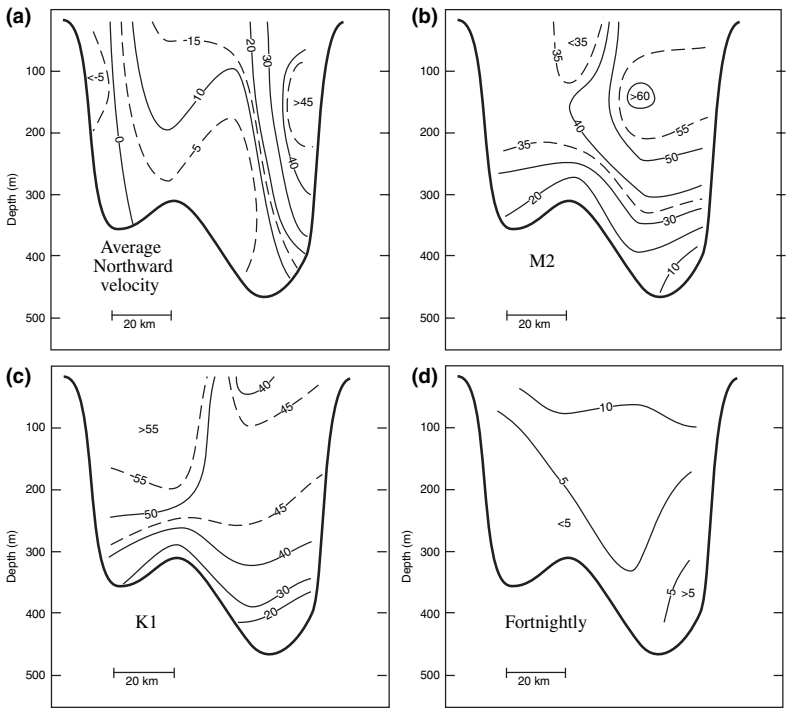

Figure 11. (a) Contours of mean northward velocity (cm s^{-1}). (b) Contours of the mean amplitude of the major axis of the tidal ellipse of M_2 (cm s^{-1}). (c) Contours of the mean amplitude of the major axis of the tidal ellipse of K_1 (cm s^{-1}). (d) Contours of amplitude of the least-squares sinusoidal fit to the northward velocity component (cm s^{-1}). All averages are over the period May 2001–2003.

Figure 12. Low-pass filtered time series of currents at the four moorings sites in Amukta Pass. Amukta-1 is on the east side of the pass and Amukta-4 is on the west side. The average depth of the measurements is indicated.

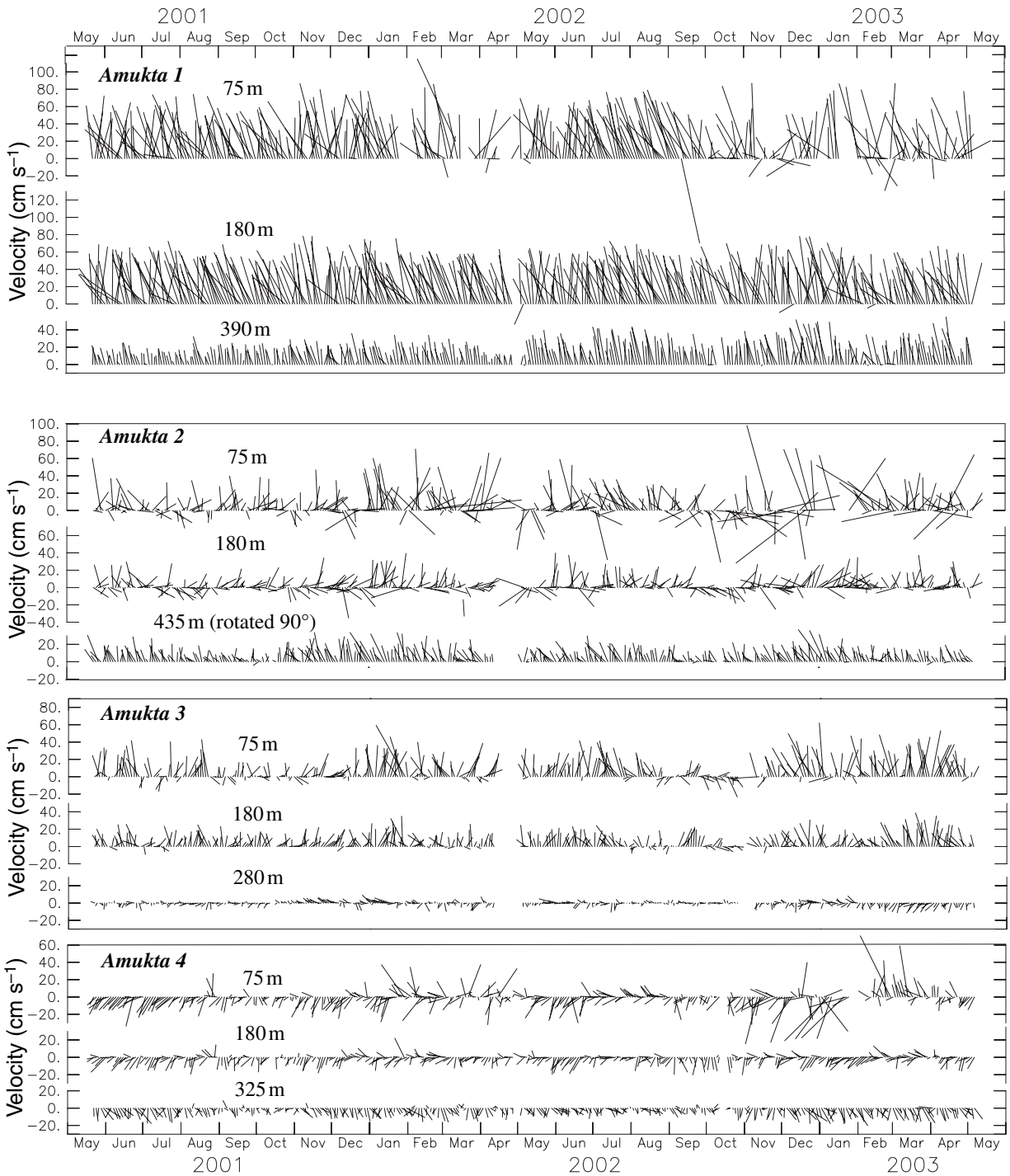

ADCPs provide the best type of data to measure transport since they measure currents throughout the water column in discrete bins. Unfortunately, there were problems in two of the passes (Akutan and Tanaga) that hindered a calculation of transport. Tanaga Pass is relatively wide and the ADCP there was on the slope at the eastern edge of this pass and, so, does not provide a good estimate of transport through

the pass. Thus, no estimate was made for Tanaga. The ADCP in Akutan Pass was also deployed at a poor location (too far north) to determine transport. The RCM9s at the southern site failed early on each deployment and, thus, do not provide a continuous time series; however, they do provide an indication of magnitude of transport. Using the three records from the southern site and assuming that this is a good estimate of barotropic velocity throughout the 80 m depth and 10 km width of the pass gives an estimated transport of 0.1×10^6 m^3 s^{-1}. This transport is similar to the barotropic transport in Unimak Pass (Stabeno *et al.*, 2002), but as in Unimak, there is a significant baroclinic component that is not included in this estimate.

The position of the ADCP at the southern mooring in Seguam Pass was near the centre of the pass and should provide a reasonable time series of transport. Following the procedure outlined in the methods section, a time series of transport was calculated (Fig. 13, top panel). The transport was northward, with a few short periods (<3 days) of southward flow, resulting in an average transport of $\sim 0.4 \times 10^6$ m^3 s^{-1}. The magnitude varied on fortnightly time scales. There is some indication of a seasonal cycle with maximum transports occurring in the winter, but, with data collected during a single winter, the seasonal cycle is not definitive.

The most reliable estimates of transport come from the four moorings across Amukta Pass. Again, following the procedure outlined in the methods section, a time series of transport was calculated over the 2-year period (Fig. 13, middle panel). The largest error in this estimate is in the upper 50 m of the water column where flow is strong and there is little data. Transport is consistently northward with only a few short periods of weak southward flow, resulting in an average northward transport of $\sim 4 \times 10^6$ m^3 s^{-1}. Variability at fortnightly time scales dominates the time series. In addition, there is evidence of variability on longer time scales of several months. To examine this, a simple box filter (55 points) was applied to the 6-hourly time series (Fig. 13, lower panel). An estimate of transport was also calculated at the Alaskan Stream mooring in the upper 500 m using a width of 20 km. The two ~50-day periods of high transport in Amukta are clearly related to transport at the Alaskan Stream site (Fig. 13). The large discrepancy in Feb-

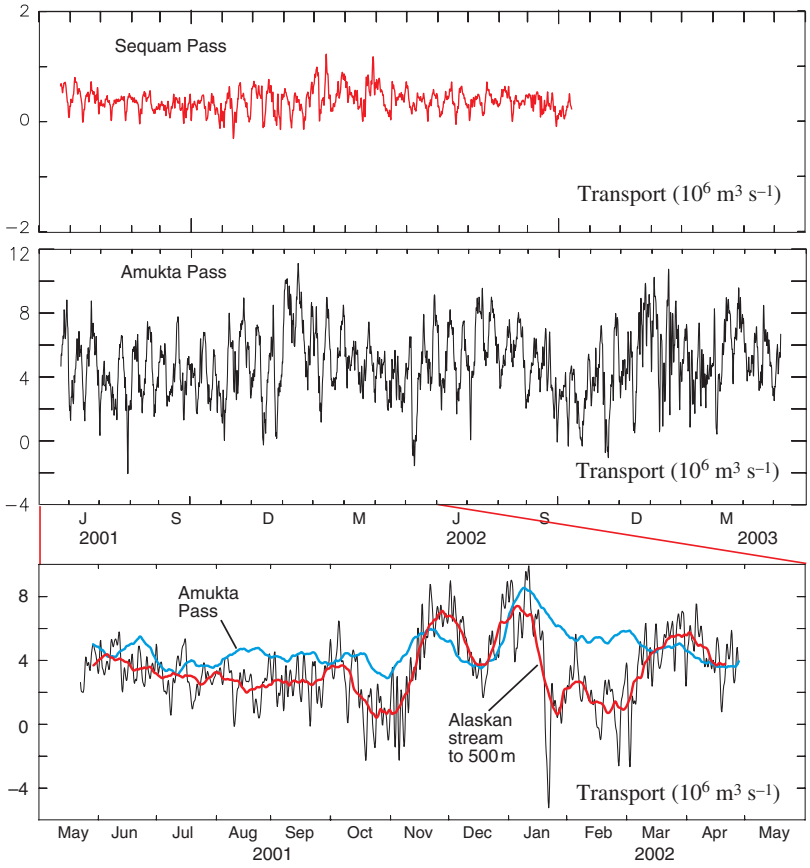

Figure 13. Top panel: Low-pass filtered transport at Seguam Pass. Middle panel: Low-pass filtered transport at Amukta Pass. Bottom panel: Low-low-pass (55-point running mean applied to the low-pass filtered data shown in the middle panel) filtered transport in Amukta Pass (blue). Low-pass filtered transport (black) in the upper 500 m at the Alaskan Stream mooring site shown in Fig. 2. Low-low-pass filtered (55 point running mean) of the transport in the upper 500 m of the Alaskan Stream (red line).

ruary and March 2002 may be due to the unusually strong northward flow at the Amukta-4, thus increasing the total northward transport through Amukta Pass. Because of the strong fortnightly signal that dominates the variability in transport through Amukta Pass, it is difficult to detect if the variability in transport in the Alaska Stream at higher frequencies impacts the flow in Amukta Pass.

Vertical mixing in the passes

The strong tidal currents through the passes provide ample energy to mix the water column. Moorings designed to examine mixing were deployed in two locations – the northern site in Akutan Pass and the southern site in Seguam Pass. Even though salinity is important in controlling density at these temperatures, we use temperature as a surrogate for water-column structure since it is easier to measure, with fewer errors and less instrument drift than occurs in measuring salinity.

In Akutan Pass, temperature was measured at four depths (Fig. 14). A plot of low-pass filtered time series shows an increase in temperature throughout the water column reaching a maximum in August. Clearly, with the steady increase in temperature at all depths, mixing must be occurring at some location on the shelf. An examination of the unfiltered (hourly) data shows that the strength of stratification was associated with the tidal cycles. When the flow was northward, the bottom temperature increased, with the water column becoming less stratified. When the tidal currents reversed and flowed southward, the bottom temperatures decreased and stratification increased. This is consistent with the hypothesis that mixing occurs south of the mooring site over the shallow sill of the pass, and mixed water is then advected northward past the mooring site. If mixing were occurring locally, then the water column would be least stratified when the currents were strongest.

The second mooring site at which stratification was examined was near the southern site in Seguam Pass (Fig. 15). There were five temperature sensors on the mooring (the sixth one at 30 m was lost when the mooring failed). The low-pass filtered time series show a better-mixed water column than was observed at Akutan, even though Akutan is shallower than Seguam Pass. As the summer progressed, the upper water column warmed and stratification increased. The temperature changed on fortnightly time scales, with the warmest temperature and greatest stratification occurring when the low-pass filtered, near-bottom current speed was at a minimum. Examination of the unfiltered data during a 6-day period in June shows that the temperature and magnitude of stratification varied with

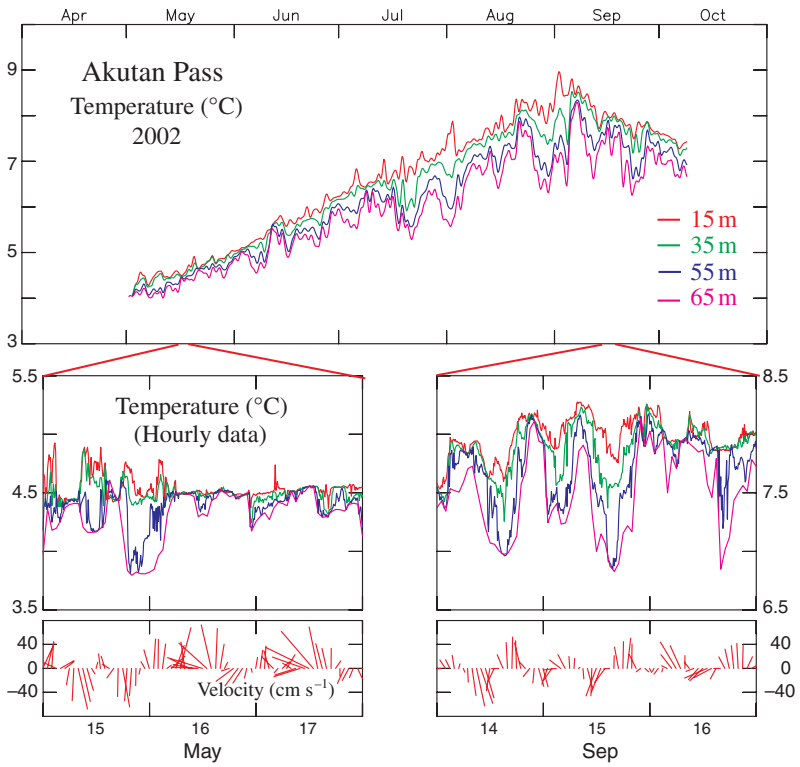

Figure 14. Low-pass filtered temperatures measured at the northern Akutan mooring. Expansions of the time series during two periods show the raw (hourly and 10 min) temperature data and the hourly velocity records.

Figure 15. Low-pass filtered temperatures measured at the southern Seguam mooring. Expansions of the time series during one period showing the raw (hourly and 10 min) temperature data and the hourly velocity records.

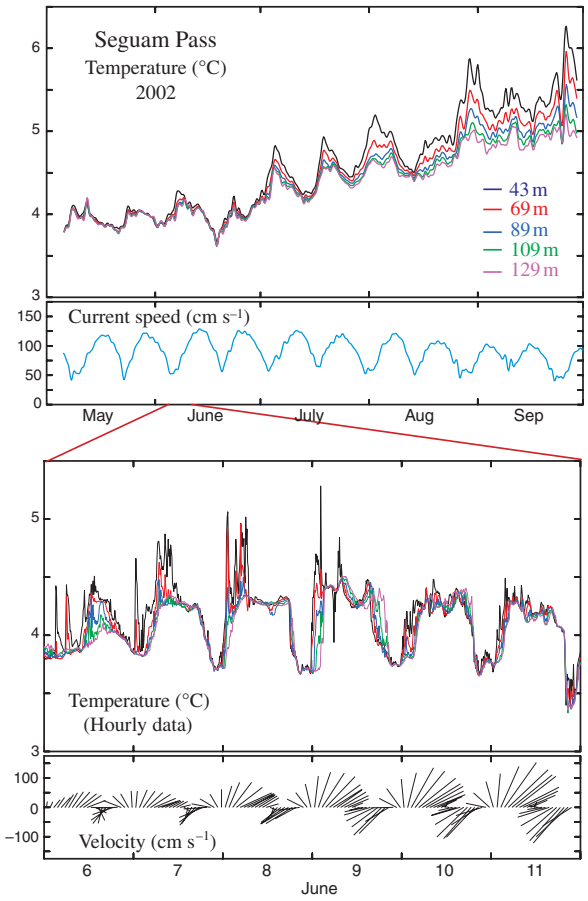

the diurnal tidal cycle. During periods of southward flow, the water column was less stratified than during periods of northward flow. Once again, this is consistent with the idea that mixing occurs in the shallow part of the pass. During periods of northward flow, water has just entered the shelf and is only partially mixed. During periods of southward flow, the water is being advected from the shallow, central part of the pass to the deeper portions of the pass, and so it is well mixed.

DISCUSSION AND CONCLUSIONS

The Aleutian passes provide a porous boundary through which water, heat, salt, and nutrients flow. The dynamics of the passes varied according to their depth and width. Akutan, a narrow shallow pass, had similar water properties and transport characteristics to those in Unimak Pass. The water flowing northward through Akutan is at least partially derived from the ACC.

Currents and water properties in Seguam Pass and Tanaga Pass, with sill depths and east–west extent 2–6 times that of Akutan, differed markedly from that in Akutan. Northward flow was stronger with fewer reversals. In addition, the time series of currents and salinity were modified by a pronounced fortnightly signal.

The transport through Amukta Pass, at 4×10^6 m^3 s^{-1}, was approximately five times as large as baroclinic estimates made from hydrographic survey (Reed and Stabeno, 1997). There are many possible causes for this, but the most likely are: a strong barotropic component at the eastern mooring (and to a lesser extent at Amukta-2), increasing the transport by $\sim 1.5 \times 10^6$ m^3 s^{-1}; the eastern-most hydrographic station was too far west, thereby missing a significant portion of the high-speed jet along east side of the pass, which would contribute $\sim 1 \times 10^6$ m^3 s^{-1} to the transport; and finally, non-linear tidal interactions resulting in strong fortnightly tides.

The position and strength of the Alaskan Stream influenced the magnitude of the flow through Amukta Pass and probably through the other large passes as well. When the Alaska Stream weakened or meandered offshore, the transport weakened in Amukta Pass. The mechanisms that controlled transport on shorter time scales are less clear because of the strong fortnightly signal. There does not appear to be a strong relationship with local wind forcing.

How the passes contribute to the Bering Sea current and water properties differs according to their size. Passes with depths between 120 and 200 m, such as Seguam Pass and perhaps Tanaga, are most efficient in mixing nutrients upwards, since their sills are deeper than the nutricline and yet are shallow enough so that the strong tidal currents mix the water column vertically, thus introducing those nutrients into the euphotic zone. These passes provide moderate transport (0.4×10^6 m^3 s^{-1}) and large amounts of nutrients in the upper water column. There are several passes, such as Adak Strait (~177°W), Atka Pass (~175.5°W) and Samalga Pass (~170°W), of dimensions similar to Seguam.

The sills of shallow passes such as Akutan are above the nutricline, and, thus, high concentrations of nutrients are unavailable for mixing. So, the smaller passes provide both limited nutrients and transport into the Bering Sea, although Unimak Pass introduces water directly onto the eastern Bering Sea shelf (Stabeno *et al.*, 2002).

In contrast to the shallow passes, deep passes such as Amukta Pass are too deep to mix completely in the vertical, thus they do not introduce high concentra-

tions of nutrients into the euphotic zone. Large passes such Amukta Pass, and likely Amchitka Pass, Bulduir Pass and Near Strait, contribute most of the transport to the Bering Sea gyre, and, hence, are an important source of heat.

The nutrients introduced through mixing in the passes and then advected northward are critical to Bering Sea ecosystem. During summer, primary production consumes the nutrients along the north side of the Aleutian Islands in the upper ~40 m. During the following winter, strong storms mix the water column to >150 m (Cokelet and Stabeno, 1997; Johnson *et al.*, 2004), thus introducing the nutrients into the euphotic zone that were mixed in the passes for use the following spring. During winter, high concentrations of nutrients are introduced into the upper 100 m and advected northeastward along the slope of the broad eastern Bering Sea shelf. These nutrients are then advected onto the shelf through wind-driven currents and instabilities, supplying the nutrients to support the next summer's production (Stabeno *et al.*, 1999).

The passes in the Aleutian Arc play a critical role in the Bering Sea ecosystem, especially the moderate size passes, such as Seguam. Locally, the moderate and smaller passes support large number of foraging birds and mammals (Ladd *et al.*, 2005b), unlike Amukta Pass which had fewer flocks of birds and mammals. On large scales, the transport through the passes are the source of essential nutrients and heat necessary to maintain the high productivity of the Bering Sea ecosystem.

ACKNOWLEDGEMENTS

We thank W. Parker, C. Dewitt, W. Floering and the officers and crew of the NOAA ship *Miller Freeman* for ensuring the successful deployment and recovery of the moorings. This research in contribution No. 2660 from NOAA/Pacific Marine Environmental Laboratory and contribution FOCI-L528 to NOAA's Fisheries Oceanography Coordinated Investigations and was supported by the Joint Institute for the Study of the Atmosphere and Ocean under cooperative agreement NA17RJ1232, Contribution No. 1085.

REFERENCES

Cokelet, E.D. and Stabeno, P.J. (1997) Mooring observations of the thermal structure, salinity, and currents in the SE Bering Sea basin. *J. Geophys. Res.* **102:**22947–22964.

Favorite, F. (1974) Flow into the Bering Sea through Aleutian island passes. In: *Oceanography of the Bering Sea with Emphasis on Renewable Resources*. D.W. Hood & E.J. Kelley (eds) Fairbanks: Occasional Publication No. 2, Institute of Marine Science, University of Alaska, pp. 3–37.

Favorite, F., Dodimead, A.J. and Nasu, K. (1976) *Oceanography of the Subarctic Pacific Region, 1960–71*. International North Pacific Fisheries Commission, Bull. No. 33, p. 187.

Johnson, G.C., Stabeno, P.J. and Riser, S.C. (2004) The Bering Slope Current System revisited. *J. Phys. Oceanogr.* **34:**384–398.

Ladd, C., Hunt, G.L. Jr., Mordy, C.W., Salo, S. and Stabeno, P.J. (2005a) Marine environment of the central and eastern Aleutian Islands. *Fish. Oceanogr.* **14 (Suppl. 1):**22–38.

Ladd, C., Jahncke, J., Hunt, G. L. Jr., Coyle, K.O. and Stabeno, P.J. (2005b) Hydrographic features and seabird foraging in Aleutian Passes. *Fish. Oceanogr.* **14 (Suppl. 1):**178–195.

Mordy, C.W., Stabeno, P.J., Ladd, C., Zeeman, S., Wisegarver, D.P., Salo, S.A. and Hunt, G.L. Jr. (2005) Nutrients and primary production along the eastern Aleutian Island Archipelago. *Fish. Oceanogr.* **14 (Suppl. 1):**55–76.

Reed, R.K. (1990) A year-long observation of water exchange between the North Pacific and the Bering Sea. *Limnol. Oceanogr.* **35:**1604–1609.

Reed, R.K. and Mordy, C.W. (1999) Bering Sea deep circulation water properties and geopotential. *J. Mar. Res.* **57:**763–773.

Reed, R.K. and Stabeno, P.J. (1994) Flow along and across the Aleutian ridge. *J. Mar. Res.* **52:**639–648.

Reed, R.K. and Stabeno, P.J. (1997) Long-term measurements of flow near the Aleutian Islands. *J. Mar. Res.* **55:**565–575.

Schumacher, J.D., Pearson, C.A. and Overland, J.E. (1982) On exchange of water between the Gulf of Alaska and the Bering Sea through Unimak Pass. *J. Geophys. Res.* **87:**5785–5795.

Stabeno, P.J., Reed, R.K. and Schumacher, J.D. (1995) The Alaska Coastal Current: continuity of transport and forcing. *J. Geophys. Res.* **100:**2477–2485.

Stabeno, P.J., Schumacher, J.D. and Ohtani, K. (1999) The physical oceanography of the Bering Sea. In: *Dynamics of the Bering Sea: A Summary of Physical, Chemical, and Biological Characteristics, and a Synopsis of Research on the Bering Sea*. T.R. Loughlin & K. Ohtani (eds) University of Alaska Sea Grant, AK-SG-99-03, North Pacific Marine Science Organization (PICES), pp. 1–28.

Stabeno, P.J., Reed, R.K. and Napp, J.M. (2002) Transport through Unimak Pass, Alaska. *Deep-Sea Res. II: Topical Stud. Oceanogr.* **49:**5919–5930.

Stabeno, P.J., Bond, N.A., Hermann, A.J., Kachel, N.B., Mordy, C.W. and Overland, J.E. (2004) Meteorology and oceanography of the northern Gulf of Alaska. *Cont. Shelf Res.* **24:**859–897.